Duan *et al.*
European Journal of Medical Research (2025) 30:423
https://doi.org/10.1186/s40001-025-02673-6

European Journal of Medical Research

RESEARCH Open Access

Dosimetric comparison of two linear accelerators for lung cancer SBRT using IMRT dose delivery technique: VenusX vs. Edge

Yanhua Duan[1,2†], Shanshan Zhong[3†], Aihui Feng[1,2], Qing Kong[1] and Zhiyong Xu[2*]

Abstract

Background The VenusX and Edge accelerators are two commercially available systems used for lung stereotactic body radiation therapy (SBRT) with Intensity-Modulated Radiation Therapy (IMRT) techniques.

Methods A retrospective analysis was conducted on 40 lung cancer patients treated with the Edge accelerator. Treatment plans using both the Edge ($Plan_{Edge}$) and VenusX ($Plan_{VX}$) accelerators were generated and evaluated using various dosimetric metrics, employing statistical analyses to identify significant differences.

Results For planned target volume (PTV), Plan $_{VX}$ outperformed $Plan_{Edge}$ across the entire cohort, achieving a higher D2 dose (76.84 vs 75.56 Gy, $p = 0.005$), and showing significant improvements in conformity index (0.84 vs 0.80), homogeneity index (0.50 vs 0.47), and gradient index (5.12 vs 5.62), all with $p < 0.001$. Plan $_{VX}$ also recorded a lower $D_{2\,cm}$ (27.27 vs 27.87 Gy, $p = 0.004$). Subgroup analyses revealed significant enhancements in conformity index (CI), homogeneity index (HI), and gradient index (GI) for both single and multi-target lesion patients, with multi-target also seeing a notably lower $D_{2\,cm}$. regarding organs at risk (OARs), Plan $_{VX}$ significantly reduced lung mean dose (D_{mean}) (3.85 to 3.60 Gy), V_5 (16.88% to 15.61%), and V_{20} (5.04% to 4.63%), along with improvements in the great vessels' D_{mean} and max dose (D_{max}), and esophagus' D_{max} across all patients. Single-lesion patients saw consistent lung improvements, while multi-lesion patients experienced significant lung reductions and enhancements in great vessels' and esophagus' metrics.

Conclusions In conclusion, both $Plan_{VX}$ and $Plan_{Edge}$ achieved treatment plans that met the dosimetric criteria defined by the RTOG guidelines. While Plan $_{VX}$ exhibited improved values in CI, HI, and GI, these findings reflect observed dosimetric differences rather than definitive evidence of clinical superiority. Further prospective studies are warranted to evaluate the clinical relevance of these differences.

Introduction

Stereotactic body radiation therapy (SBRT) is a tumor treatment technology widely used in clinics, providing high-precision ablative therapy to tumors while minimizing damage to organs at risk (OARs) [1]. Many studies have confirmed that SBRT can achieve outcomes similar to surgery in patients with early-stage non-small cell lung cancer (NSCLC), suggesting it as the preferred option for NSCLC patients who cannot tolerate surgery [2]. SBRT is also used for local control in other stages of cancer [3].

†Yanhua Duan and Shanshan Zhong have contributed equally to this work.

*Correspondence:
Zhiyong Xu
xzyong12vip@sina.com
[1] Institute of Modern Physics, Fudan University, Shanghai, China
[2] Department of Radiation Oncology, Shanghai Chest Hospital, Shanghai Jiao Tong University School of Medicine, Shanghai, China
[3] Department of Radiation Oncology, Zhongshan City People's Hospital, Guangdong, China

Technological advancements have significantly improved the effectiveness of accelerator-based SBRT. Its delivery times are notably shorter than devices like the Gamma Knife [4, 5]. These advancements also include techniques like 4DCT, gating, and breath-hold. These methods enhance treatment accuracy by accounting for tumor motion and ensuring precise targeting. Consequently, there has been a growing preference for accelerator-based SBRT among doctors and patients. Multiple studies [2] show accelerator-based SBRT yields favorable prognoses. This requires achieving highly conformal targets and steep dose gradients. These features ensure that surrounding healthy tissues are minimally exposed to radiation, thereby reducing the risk of complications such as pneumonia and fibrosis. This approach not only ensures effective tumor ablation but also improves overall survival rates and the quality of life for patients [6].

Treatment planning quality depends on multiple factors. These include the accelerator's mechanical design (e.g., the multi-leaf collimator, or MLC) and software designs. The latter encompasses beam models, machine models, and calculation algorithms in the treatment planning system [7, 8]. MLCs are critical components in modulating the radiation beam to conform to the complex geometry of the tumor. They work with other mechanical components to reduce radiation leakage. This helps protect surrounding normal tissues. They also work with the treatment planning system's advanced modeling capabilities. This synergy ensures accurate targeting and safe delivery, especially for SBRT.

The VenusX accelerator (LinaTech (Beijing) TF Medical Science and Technology Co., Ltd., Beijing, China) is a newly developed radiation therapy system, while the Edge accelerator (Varian Medical Systems, Palo Alto, CA) is a widely used and established system in clinical practice. Both are utilized for delivering high-precision SBRT, providing a basis for their comparative evaluation. In this work, we retrospectively enrolled a group of lung cancer patients undergoing SBRT with single and multiple targets, generating SBRT plans for the Edge™ linear accelerator (Varian Medical Systems, Palo Alto, CA) and VenusX accelerator.

Both VenusX and Edge accelerators can deliver high-precision SBRT. However, systematic dosimetric comparisons between new orthogonal dual-layer MLC systems and conventional single-layer systems remain scarce for lung cancer. This represents a critical knowledge gap, as the design of the MLC can significantly influence the dose conformity and normal tissue sparing—factors that are essential for effective SBRT treatment. To address this gap, the present study evaluates and compares the dosimetric performance of the VenusX and Edge systems under identical planning parameters. Our results demonstrate that the VenusX dual-layer MLC system offers promising dosimetric results in both single- and multi-lesion cases, offering a potential treatment option for lung cancer SBRT patients.

Materials and methods

Patient data

This study conducted a retrospective analysis of 40 lung cancer patients who underwent SBRT treatment using the Edge accelerator at our institution from May 2019 to June 2021. Among these patients, 22 had single-target lesions, while 18 had multi-target lesions. At the onset of the study, all selected patients had signed informed consent forms and had completed their radiation therapy. The native ethics committee approved this study (committee's reference number: xxxx), recognizing its minimal risk due to its retrospective nature.

Patients were scanned using the Siemens Somatom Definition AS computed tomography (CT) Scanner System (Siemens Healthcare, Erlangen, Germany) to acquire both free-breathing CT and four-dimensional computed tomography (4DCT) image sets. Expert radiation oncologists delineated all targets on the MIM Maestro Station (MIM Vista Corp, Cleveland, OH). The gross tumor volume (GTV) was defined across all ten phases of the 4DCT. Subsequently, these ten GTVs were merged to form the internal target volume (ITV). The planned target volume (PTV) was obtained by expanding the ITV by 0.5 cm in all three dimensions. An independent radiation oncologist reviewed and approved all delineations prior to their use in treatment planning.

Treatment planning

In addition to plans based on the Edge accelerator ($Plan_{Edge}$), a retrospective SBRT plan based on the VenusX accelerator ($Plan_{VX}$) was also created for each patient. Treatment plans were generated using the patients'average CT scans. Each plan was designed by an experienced physicist who was unaware of the planning processes for the other technology, and subsequently reviewed by an independent senior physicist. For all treatment plans, the prescribed dose's PTV coverage was standardized to include 95% of the volume. PTV and OAR compliance adhered to guidelines established by the Radiation Therapy Oncology Group (RTOG) [9–11].

For single-lesion patients, the isocenter was placed at the geometric center of the target. For multi-lesion patients, a single-isocenter technique was used, with the isocenter positioned near the geometric center of all targets and adjusted as necessary to optimize coverage and minimize dose to surrounding organs-at-risk (OARs). This approach was consistently applied across all plans.

Figure 1 presents the conceptual layout and machine profiles of the VenusX accelerator (A, B, and C) and the Edge accelerator (D, E, and F). Panels A and D showcase the external views of the accelerators, panels B and E illustrate the components within the treatment heads, and panels C and F provide detailed vertical views of the MLC configurations.

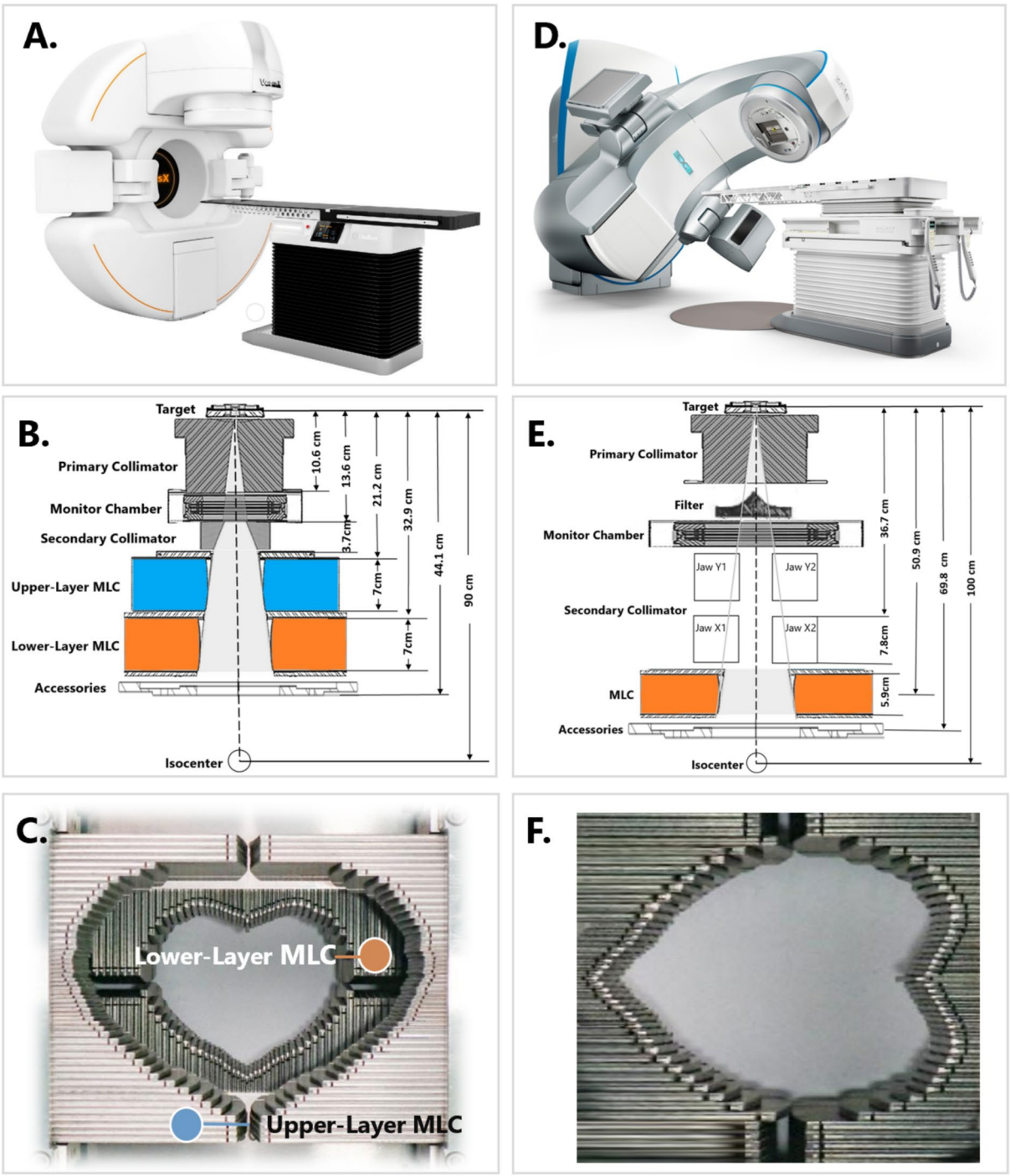

Fig. 1 Concept layout and machine profile for Venus X accelerator. **A** and **D** External views of the VenusX and Edge accelerators, respectively. **B** and **E** Structural components of the gantry heads of the VenusX and Edge accelerators. **C** and **F** Top-down views showing the detailed configuration of the MLCs in the VenusX and Edge systems

Plan $_{Edge}$ utilized the auto-planning module of the Pinnacle treatment planning system (TPS) (Version 9.10, Philips Radiation Oncology Systems, Fitchburg, WI, USA) tailored for an Edge™ linear accelerator. The Edge accelerator features a structured treatment head comprising several key components designed for precise radiation delivery. The beam originates from the target, followed by initial shaping through the primary collimator. The monitor chamber measures and regulates the radiation dose. Beam modulation is further refined by the secondary collimator, consisting of jaws (Jaw Y1, Jaw Y2, Jaw X1, and Jaw X2), which dynamically shape the radiation field. Below this, the high-definition (HD) 120 multi-leaf collimator (MLC) provides additional precision in conforming the beam to the target shape. The HD 120 MLC features 120 leaves, with the central 32 pairs projecting a leaf width of 2.5 mm at the isocenter plane, and the 14 pairs on either side projecting a width of 5.0 mm [12]. Accessories at the base of the head are used for patient-specific treatment requirements. The total source-to-axis distance (SAD) is 100 cm, with intermediate distances such as 50.9 cm to the monitor chamber, and 69.8 cm to the secondary collimator contributing to the beam's modulation and accuracy. Each plan incorporated ten or more 6 MV flattening filter-free (FFF) beams, with gantry angle intervals maintained at either 15 or 20 degrees between beams. Modifications to collimator and couch angles were tailored to meet individual patient requirements. Dose calculations were performed using the collapsed cone convolution (CCC) algorithm with a grid size of 2.0 mm.

Plan $_{VX}$ was specifically developed for use with the VenusX accelerator, an innovative medical electron linear accelerator distinguished by its unique orthogonal dual-layer MLC design. The VenusX system operates exclusively in a 6 MV FFF photon mode, optimizing beam delivery for high-precision treatments. The VenusX accelerator features an advanced treatment head design tailored for precise dose delivery. The radiation beam originates at the target and is initially shaped by the primary collimator. The monitor chamber measures and regulates the radiation dose, after which the beam is further refined by the secondary collimator. A standout feature of the VenusX is its dual-layer MLC system, consisting of 51 pairs of leaves in each layer. The upper-layer MLC, with leaves moving in the Y direction (parallel to the gantry rotation axis), has leaf thicknesses of 6 mm at the center and 12 mm at the edges. The lower-layer MLC, with leaves moving in the X direction (perpendicular to the gantry rotation axis), features leaf thicknesses of 4 mm at the center and 8 mm at the edges. This orthogonal arrangement enhances beam modulation precision and provides superior dose conformity to the target volume. The dual-layer MLC is strategically positioned, with the upper layer located 32.9 cm from the target and the lower layer at 44.1 cm. The total source-to-axis distance (SAD) is 90 cm. Additionally, customizable accessories at the base of the treatment head facilitate patient-specific treatment requirements. Treatment planning for the VenusX system was conducted using the TiGRT treatment planning system (TPS, V2.0.10.639, Suzhou LinaTech Medical Science and Technology Co., Ltd., Suzhou, China). IMRT plans were individually designed by experienced physicists, employing beams spaced at 15–20-degree intervals. Couch angles were tailored to the specific needs of each patient, with minimal collimator adjustments required due to the unique orthogonal dual-layer MLC design. Plan optimization utilized the fluence map optimization (FMO) algorithm, with dose calculations performed using the Monte Carlo (MC) algorithm and a 2 mm dose grid resolution.

To ensure consistency, all plans in this study were created by the same experienced planner using consistent constraints and optimization objectives. This approach minimizes the influence of planner preference or experience, ensuring that the observed dosimetric differences are primarily due to the machine-specific characteristics, such as MLC design.

Evaluation tools

As shown in Table 1, the metrics for targets include the doses received by the hottest 2%, the coolest 98%, and 50% of the PTV (D_2, D_{98}, D_{50}), the conformity index (CI), homogeneity index (HI), gradient index (GI), and the maximum dose at 2 cm away from the PTV in all directions ($D_{2\ cm}$). The CI, GI, and HI were defined as follows [6, 13]:

$$CI = V_{T,Rx}^2/(V_T * V_{Rx}) \quad (1)$$

$$GI = V_{50\%Rx}/V_{Rx} \quad (2)$$

$$HI = (D_2 - D_{98})/D_{50} \quad (3)$$

where $V_{T,Rx}$ is the volume of the target receiving a dose equal to or greater than the prescription dose, V_T is the target volume, and V_{Rx} is the volume receiving a dose equal to or greater than the prescription dose, and $V_{50\%Rx}$ is the volume receiving a dose equal to or greater than half the prescription dose. CI ranges from 0 to 1, with CI 1 indicating optimal conformability. A lower GI value indicates a quicker dose fall-off in normal tissue away from the target.

The dosimetric metrics for OARs are also detailed in Table 1. The evaluated OARs include the total lung, heart, great vessels, spinal cord, esophagus, and trachea. The

Table 1 Metrics used in different structures

Metrics	PTV	Total lung	Heart	Great Vessels	Spinal Cord	Esophagus	Trachea
D_2	√						
D_{98}	√						
D_{50}	√						
CI	√						
HI	√						
GI	√						
$D_{2\,cm}$	√						
V_5		√					
V_{20}		√					
D_{mean}		√	√	√			
D_{max}				√	√	√	√

metrics for evaluation include D_{mean} and D_{max}, representing the mean and maximum doses covering a tissue, and V_5 and V_{20}, which denote the percentage volume receiving a dose level of at least 5 Gy and 20 Gy, respectively.

Statistical analysis

A two-tailed paired t-test was performed to compare paired data, with statistical significance defined as a two-sided p-value less than 0.05. All analyses were conducted using R version 4.0.2 (R Foundation for Statistical Computing, Vienna, Austria).

Results

Patients

Detailed patient characteristics in this study are tabulated in Table 2. Our study involved 40 patients with a median age of 66 years (range 55–86). The cohort was 60% male and 40% female. Histologically, 22.5% had squamous cell carcinoma and 77.5% had adenocarcinoma. Clinically, 55% were stage I, 35% stage II, 7.5% stage III, and 2.5% stage IV. Tumors were located in the left lung (62.5%), right lung (30%), or both (7.5%), with a median target volume of 5.64 cm^3 (range 0.61–20.45 cm^3). Half of the patients had a single tumor lesion, while the remainder had multiple, with 75% peripheral, 15% central, and 10% both tumor types. Prescription doses were 60 Gy (15%), 50 Gy (75%), and 30 Gy (10%).

Case example

Figure 2 presents beam's eye view (BEV) examples for patients with single target (A, B) and multiple targets (C, D and E, F). It can be seen that compared to Plan $_{Edge}$, Plan $_{VX}$ allows for more refined field modulation.

Table 2 Patient characteristics

Characteristic	Number (range/proportion)
Age	
Median, year	66 (55–86)
Sex	
Male	24 (60%)
Female	16 (40%)
Histology	
Squamous cell carcinoma	9 (22.5%)
Adenocarcinoma	31 (77.5%)
Clinical stage	
I	22 (55%)
II	14 (35%)
III	3 (7.5%)
IV	1 (2.5%)
Tumor location	
Left lung	25 (62.5%)
Right lung	12 (30%)
Left lung & Right lung	3 (7.5%)
Target volume	
Median, cm^3	5.64 (0.61–20.45)
Number of Lesions	
1	20 (50%)
2	16 (40%)
3	3 (7.5%)
4	1 (2.5%)
Tumor Type	
Peripheral	30 (75%)
Central	6 (15%)
Peripheral & Central	4 (10%)
Prescription dose (Gy)	
60	6 (15%)
50	30 (75%)
30	4 (10%)

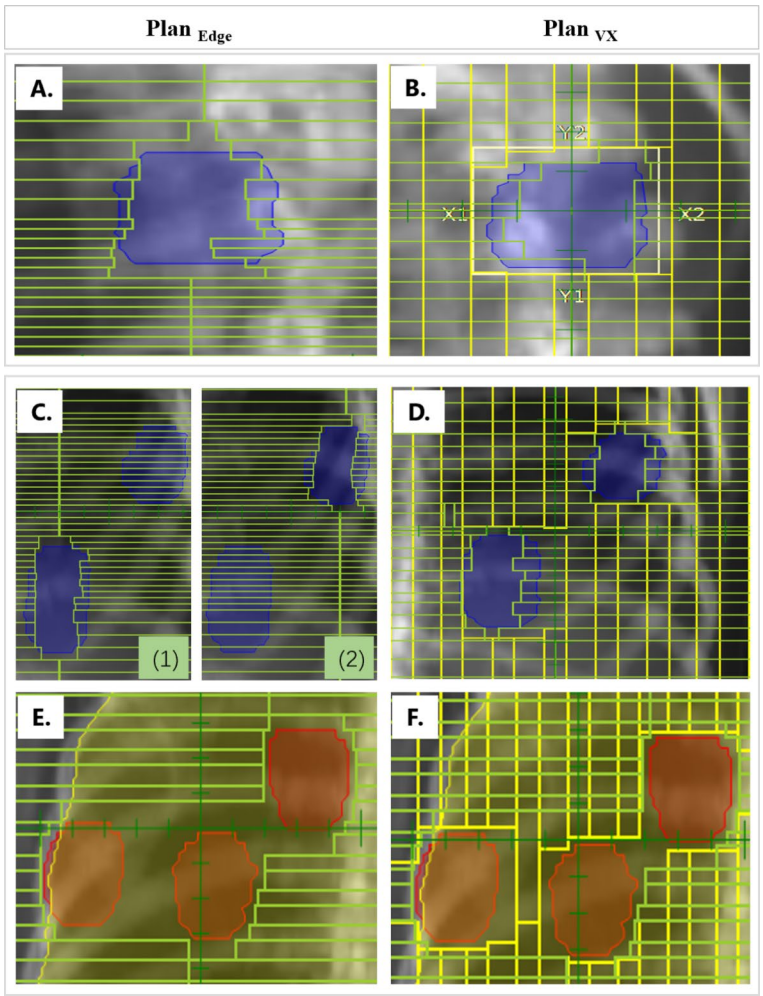

Fig. 2 Beam's eye view (BEV) examples for patients with single and multiple targets. **A** and **B** Representative single-lesion SBRT plans generated using the Edge and VenusX systems. **C** and **D** Multi-lesion SBRT plans created with the Edge and VenusX systems. **E** and **F** SBRT plans for another case using the Edge and VenusX systems

Dosimetric evaluations for PTV

Table 3 shows the comparison of dosimetric parameters of PTV between $Plan_{Edge}$ and $Plan_{VX}$ for all patients, single-lesion patients, and multi-lesion patients. The results are reported as mean values with ranges in parentheses.

For the entire cohort, encompassing both single-lesion and multi-lesion patients, the Plan $_{VX}$ demonstrated a marginally higher mean D_2 dose of 76.84 Gy (range 41.85 to 104.57 Gy) compared to 75.56 Gy (range 41.35 to 100.51 Gy) for Plan $_{Edge}$, with statistical significance ($p = 0.005$). However, no significant differences were observed in the D_{98} and D_{50} doses between the two plans, with p-values of 0.363 and 0.406, respectively. Significant improvements in dosimetric quality were noted for Plan $_{VX}$ in terms of CI, HI, and GI. Specifically, Plan $_{VX}$ improved CI (mean 0.84, range 0.75 to 0.91, $p < 0.001$), HI (mean 0.50, range 0.34 to 0.66, $p < 0.001$), and GI (mean 5.12, range 2.20 to 8.60, $p < 0.001$) compared to Plan $_{Edge}$. Additionally, a slight but statistically significant difference was noted in $D_{2\ cm}$, with Plan $_{VX}$ showing a lower mean dose of 27.27 Gy (range 16.57 to 43.88 Gy) compared to 27.87 Gy (range 17.07 to 45.13 Gy) for Plan $_{Edge}$ ($p = 0.004$).

In the subgroup analysis, single-lesion patients treated with $Plan_{VX}$ exhibited a non-significant trend towards higher D_2 doses, with a mean of 81.33 Gy (range 74.68 to 88.94 Gy) compared to 80.36 Gy (range 75.63 to 84.96 Gy) for $Plan_{Edge}$ ($p = 0.126$). Similarly, no significant differences were found in the D_{98} and D_{50}. Nonetheless, $Plan_{VX}$ achieved improved CI ($p = 0.001$), and GI ($p = 0.012$), with a non-significant trend towards improvement in HI ($p = 0.058$) and D2 cm ($p = 0.151$). For multi-lesion patients, although the mean D_2 dose was slightly higher in $Plan_{VX}$ than in $Plan_{Edge}$ (77.28 Gy vs. 76.45 Gy,

Table 3 Comparison of Dosimetric Parameters of PTV Between Plan $_{Edge}$ and Plan $_{VX}$

Cohort	Metrics	$Plan_{Edge}$	$Plan_{VX}$	*p* value
All patients	D_2 *(Gy)*	75.56 (41.35–100.51)	76.84 (41.85–104.57)	0.005
	D_{98} *(Gy)*	47.07 (28.04–58.82)	46.98 (28.35–58.13)	0.363
	D_{50} *(Gy)*	59.99 (35.48–77.26)	59.51 (35.13–77.47)	0.406
	CI	0.80 (0.62–0.87)	0.84 (0.75–0.91)	< 0.001
	HI	0.47 (0.35–0.57)	0.50 (0.34–0.66)	< 0.001
	GI	5.62 (4.01–8.76)	5.12 (2.20–8.60)	< 0.001
	$D_{2\,cm}$ *(Gy)*	27.87 (17.07–45.13)	27.27 (16.57–43.88)	0.004
Single-lesion patients	D_2 *(Gy)*	80.36 (75.63–84.96)	81.33 (74.68–88.94)	0.126
	D_{98} *(Gy)*	49.06 (46.90–49.94)	49.10 (47.55–50.06)	0.704
	D_{50} *(Gy)*	63.01 (49.97–69.39)	62.75 (59.03–67.91)	0.775
	CI	0.81 (0.62–0.87)	0.85 (0.75–0.90)	0.001
	HI	0.49 (0.42–0.56)	0.51 (0.42–0.66)	0.058
	GI	5.48 (4.36–7.95)	4.89 (2.20–6.36)	0.012
	$D_{2\,cm}$ *(Gy)*	28.04 (23.41–31.72)	27.74 (23.83–30.96)	0.151
Multi-lesion patients	D_2 *(Gy)*	76.45 (41.35–100.51)	77.28 (41.85–104.57)	0.16
	D_{98} *(Gy)*	49.10 (28.04–58.82)	49.06 (28.35–58.13)	0.80
	D_{50} *(Gy)*	61.67 (35.48–77.26)	60.01 (35.13–77.47)	0.06
	CI	0.79 (0.70–0.87)	0.83 (0.77–0.91)	< 0.001
	HI	0.45 (0.35–0.57)	0.48 (0.34–0.63)	0.003
	GI	5.77 (4.01–8.76)	5.39 (3.87–8.60)	0.005
	$D_{2\,cm}$ *(Gy)*	27.65 (17.07–45.13)	26.76 (16.57–43.88)	0.011

All patients: Single-lesion patients & Multi-lesion patients

$p = 0.16$), no significant differences were observed in D_{98} and D_{50}. Notably, $Plan_{VX}$ consistently demonstrated superior CI, HI, and GI with *p*-values < 0.001, 0.003, and 0.005, respectively. The mean $D_{2\,cm}$ dose was also significantly lower in $Plan_{VX}$ (26.76 Gy) compared to $Plan_{Edge}$ (27.65 Gy, $p = 0.011$).

Figure 3 provides a more intuitive representation of the differences in PTV metrics between Plan $_{VX}$ and Plan $_{Edge}$, with the displayed box plots showing results after removing outliers at the 1% and 99% levels.

In conclusion, our analysis demonstrates that Plan $_{VX}$ generally outperforms Plan $_{Edge}$ in terms of conformity, homogeneity, and gradient indices of the targets. Notably, the advantages of Plan $_{VX}$ are more pronounced for patients with multiple lesions. These findings underscore the potential benefits of Plan $_{VX}$ in optimizing radiation therapy plans for patients with varying tumor burdens.

Dosimetric evaluations for OARs

Dosimetric comparison of Plan $_{Edge}$ and Plan $_{VX}$ revealed differential impacts across various structures in the full patient cohort, which included both single-lesion and multi-lesion cases, as outlined in Table 4.

For the entire cohort of patients, comparisons between Plan $_{Edge}$ and Plan $_{VX}$ revealed significant differences in various dosimetric metrics across different structures. Specifically, for the total lung, a significant reduction in D_{mean}, V_5, and V_{20} was observed with Plan $_{VX}$ compared to Plan $_{Edge}$, with D_{mean} decreasing from 3.85 Gy (range 1.39–13.53 Gy) to 3.60 Gy (range 1.19–12.82 Gy, $p < 0.001$), V_5 from 16.88% (range 5.32–30.04%) to 15.61% (range 4.88–30.04%, $p < 0.001$), and V_{20} from 5.04% (range 1.16–21.12%) to 4.63% (range 1.04–18.86%, $p < 0.001$). However, no significant difference was noted in heart D_{mean} (2.05 Gy vs. 1.87 Gy, $p = 0.252$). The great vessels showed a significant improvement in both D_{mean} (from 7.29 Gy to 6.63 Gy, $p = 0.006$) and D_{max} (from 24.89 Gy to 23.64 Gy, $p = 0.005$). No significant difference was found in the spinal cord's D_{max} (11.39 Gy vs. 11.11 Gy, $p = 0.427$), while the esophagus and trachea displayed significant and non-significant differences in D_{max}, respectively.

In the subgroup analysis, for single-lesion patients, Plan $_{VX}$ consistently demonstrated better performance in reducing the total lung's D_{mean} (2.86 Gy to 2.66 Gy, $p < 0.001$), V_5 (13.03% to 11.6%, $p < 0.001$), and V_{20} (3.42% to 3.15%, $p = 0.001$). No significant difference was observed in the heart's D_{mean} (1.48 Gy in both plans, $p = 0.954$). Compared to Plan $_{Edge}$, Plan $_{VX}$ showed improvements in radiation exposure to the great vessels, spinal cord, esophagus, and trachea, though not statistically significant. For the great vessels, D_{mean} improved from 6.39 Gy to 7.52 Gy (p

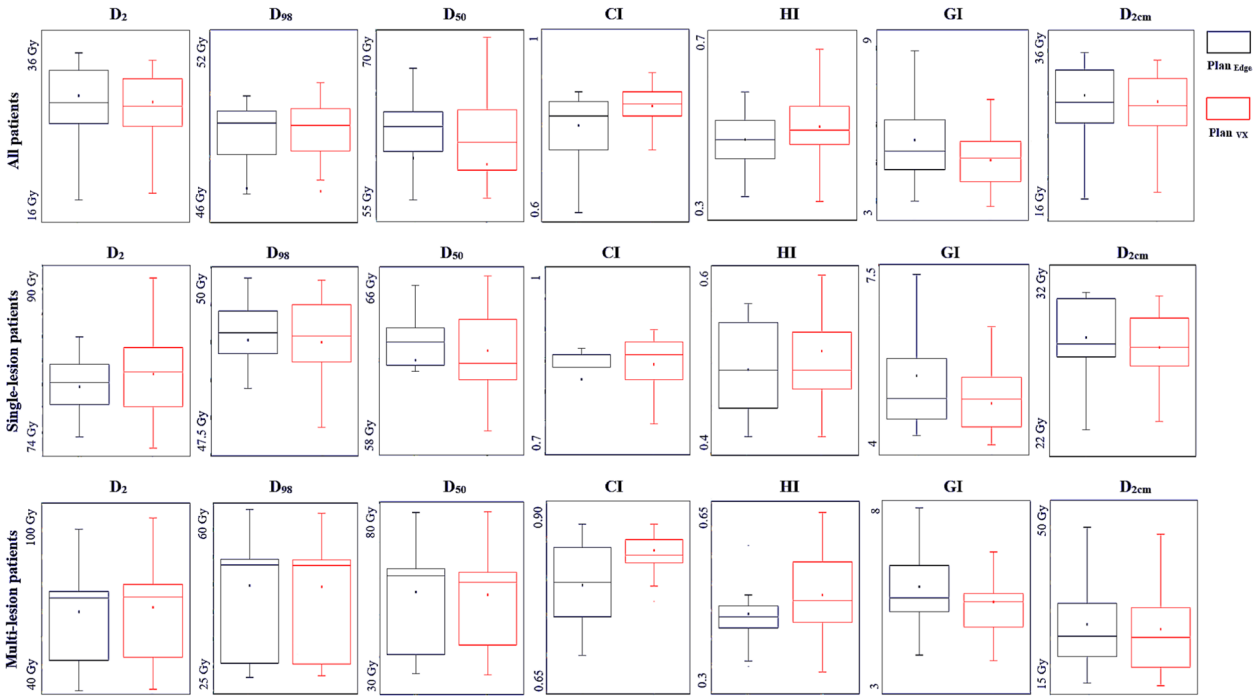

Fig. 3 Box plots for dosimetric metrics of PTV used for comparing Plan $_{VX}$ and Plan $_{Edge}$

=0.073) and D_{max} reduced from 21.26 Gy to 20.53 Gy (p =0.069). The spinal cord's D_{max} decreased from 9.31 Gy to 8.63 Gy (p =0.052). For the esophagus and trachea, D_{max} slightly decreased from 10.89 Gy to 10.61 Gy (p =0.336) and from 11.16 Gy to 11.13 Gy (p =0.914), respectively.

For multi-lesion patients, significant improvements with Plan $_{VX}$ were observed in the total lung's D_{mean} (4.95 Gy to 4.66 Gy, p< 0.001), V_5 (23.27% to 21.93%, p= 0.013), and V_{20} (6.85% to 6.27%, p= 0.002). Significant improvements were also noted in the great vessels' D_{mean} (8.68 Gy to 8.02 Gy, p= 0.009) and D_{max} (30.47 Gy to 28.43 Gy, p= 0.032). The spinal cord's D_{max} showed no significant change (13.58 Gy to 13.74 Gy, p= 0.816), whereas the esophagus showed a significant reduction in D_{max} from 13.52 Gy to 11.98 Gy (p =0.011). The heart's D_{mean} (2.73 Gy to 2.32 Gy, p= 0.249) and Trachea D_{max} (15.61 Gy to 15.11 Gy, p= 0.415) showed no significant difference, but an improvement trend.

Figure 4 illustrates the dosimetric differences in the OARs between the two plans, with the box plots representing results after removing the 1% and 99% outliers.

All treatment plans generated by both devices met the dosimetric criteria defined by the RTOG guidelines. The dosimetric evaluation highlights Plan $_{VX}$'s capacity for enhanced sparing of organs-at-risk in patients with both single and multiple lesions, especially with significant improvements in the protection of the lungs. Compared to those with single lesions, this advantage of Plan $_{VX}$ is even more pronounced in patients with multiple lesions.

Discussion

This study, by comparing the treatment plans based on the VenusX accelerator ($Plan_{VX}$) with those based on the Edge linear accelerator ($Plan_{Edge}$) in the application of SBRT for lung cancer, revealed the advantages of $Plan_{VX}$ in improving target conformality, uniformity, and gradient index, as well as in reducing the dose to OARs. Notably, for complex cases involving multi-target treatments, $Plan_{VX}$ demonstrated more significant improvements, due to its innovative design such as the orthogonal dual-layer MLC. This design optimized the spatial distribution of the dose, allowing for more precise targeting of the tumor areas while minimizing radiation exposure to surrounding normal tissues and organs at risk. These findings not only highlight the potential of the VenusX system in precise tumor targeting and protecting critical organs but also provide a technological option for SBRT treatments, especially in handling more complex multiple lesions, which is of importance for improving treatment outcomes and patient quality of life. Despite these statistical advantages, the clinical relevance and impact of such advantages remain to be determined.

A well-designed MLC should exhibit key characteristics such as low leaf transmission, minimal tong-and-groove effect, reduced penumbra, and precise leaf positioning

Table 4 Comparison of Dosimetric Parameters of OARs Between Plan $_{Edge}$ and Plan $_{VX}$

Cohort	Structure	Metrics	$Plan_{Edge}$	$Plan_{VX}$	p value
All patients	*Total Lung*	D_{mean}	3.85 (1.39–13.53)	3.60 (1.19–12.82)	< 0.001
		V_5	16.88 (5.32–30.04)	15.61 (4.88–30.04)	< 0.001
		V_{20}	5.04 (1.16–21.12)	4.63 (1.04–18.86)	< 0.001
	Heart	D_{mean}	2.05 (0.06–8.14)	1.87 (0.07–8.18)	0.252
	Great Vessels	D_{mean}	7.29 (2.57–17.65)	6.63 (2.34–18.32)	0.006
		D_{max}	24.89 (7.65–50.55)	23.64 (7.57–49.83)	0.005
	Spinal Cord	D_{max}	11.39 (2.41–36.00)	11.11 (2.27–36.15)	0.427
	Esophagus	D_{max}	11.85 (6.35–29.82)	11.11 (5.42–31.36)	0.011
	Trachea	D_{max}	12.97 (0.19–35.64)	12.74 (0.31–32.55)	0.448
Single-lesion patients	*Total Lung*	D_{mean}	2.86 (1.39–4.79)	2.66 (1.19–4.31)	< 0.001
		V_5	13.03 (5.32–21.45)	11.6 (4.88–17.78)	< 0.001
		V_{20}	3.42 (1.16–6.86)	3.15 (1.04–6.02)	0.001
	Heart	D_{mean}	1.48 (0.06–4.87)	1.48 (0.07–4.58)	0.954
	Great Vessels	D_{mean}	6.39 (2.57–17.65)	5.72 (2.34–18.32)	0.073
		D_{max}	21.26 (7.65–49.18)	20.53 (7.57–46.16)	0.069
	Spinal Cord	D_{max}	9.31 (2.90–31.02)	8.63 (2.57–29.64)	0.052
	Esophagus	D_{max}	10.89 (6.35–29.82)	10.61 (5.42–31.36)	0.336
	Trachea	D_{max}	11.16 (0.19–21.64)	11.13 (0.31–21.32)	0.914
Multi-lesion patients	*Total Lung*	D_{mean}	4.95 (1.60–13.53)	4.66 (1.50–12.82)	< 0.001
		V_5	23.27 (6.75–30.04)	21.93 (6.10–30.04)	0.013
		V_{20}	6.85 (2.36–21.12)	6.27 (1.95–18.86)	0.002
	Heart	D_{mean}	2.73 (0.13–8.14)	2.32 (0.16–8.18)	0.249
	Great Vessels	D_{mean}	8.68 (3.70–17.31)	8.02 (3.23–15.31)	0.009
		D_{max}	30.47 (8.81–50.55)	28.43 (8.12–49.83)	0.032
	Spinal Cord	D_{max}	13.58 (2.41–36.00)	13.74 (2.27–36.15)	0.816
	Esophagus	D_{max}	13.52 (6.82–21.21)	11.98 (5.59–20.87)	0.011
	Trachea	D_{max}	15.61 (0.21–35.64)	15.11 (0.35–32.55)	0.415

V_5 and V_{20} are expressed as percentages, while D_{mean} and D_{max} are in units of Gy

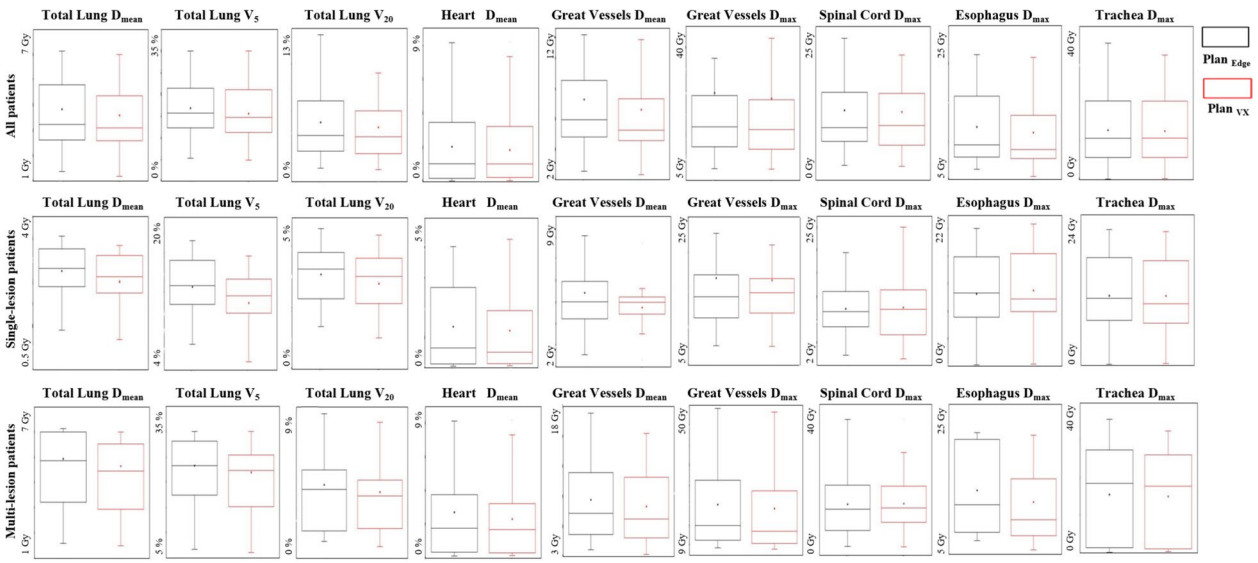

Fig. 4 Box plots for dosimetric metrics of OARs used for comparing Plan $_{VX}$ and Plan $_{Edge}$

[14]. The orthogonal dual-layer MLC of the VenusX accelerator takes these qualities further by enhancing spatial resolution compared to traditional single-layer MLCs. The orthogonal arrangement of the two layers enables finer beam modulation, reduces interleaf leakage, and improves dose conformity. This design is particularly advantageous for complex or irregular target geometries and multi-lesion treatments, ensuring sharper dose falloffs and more precise dose delivery. As highlighted by Wang et al. [15] the VenusX system demonstrates significant improvements in beam shaping accuracy and treatment plan quality, providing a strong foundation for the dosimetric advantages observed in this study.

The design and control of MLCs continue to evolve, driven by the need for greater efficiency and precision in radiation therapy. In recent years, multilayer MLC designs have emerged as a key innovation. For instance, in 2017, Varian Medical Systems introduced the Halcyon™ system, featuring a parallel dual-layer MLC that accelerates beam modulation and significantly reduces interleaf leakage. Similarly, the orthogonal dual-layer MLC studied in this research comprises two MLC layers installed orthogonally, with each layer capable of moving in perpendicular directions. This unique design may benefit radiation therapy in the following ways: (1) the corresponding leaves of the upper and lower layers collaborate at the edges of the target area, improving the conformity between the MLC shape and the target boundary; (2) the two layers of leaves shield each other during movement, reducing radiation leakage; (3) the increased effective thickness of the leaves reduces radiation transmission, minimizing the penumbral region; and (4) the orthogonal movement directions provide greater flexibility and degrees of freedom for dynamic leaf segmentation.

The dosimetric differences observed in this study cannot be solely attributed to the MLC design. Several other factors, such as variations in beam models, MLC models, calculation algorithms, optimization methods, planner preferences, source-to-axis distances (SADs), and MLC modeling in different treatment planning systems (TPSs), could also contribute to these differences. The baseline data for percentage depth dose (PDD) and profiles of these two accelerators are provided in the supplementary file. While our study highlights the unique design of the orthogonal dual-layer MLC in the VenusX system, the comparison was conducted between two commercially available systems, and the dosimetric differences reflect the combined impact of all system components.

The results of this study indicate that Plan VX demonstrates statistically significant improvements over Plan Edge in several dosimetric indicators, particularly in the treatment of patients with multiple lesions; however, the numerical differences are relatively small. In the evaluation of the PTV, $Plan_{VX}$ showed significant improvements over $Plan_{Edge}$ in terms of CI, HI, and GI. The improvement in CI indicates that $Plan_{VX}$ can provide more precise target coverage, and the improvement in GI suggests that $Plan_{VX}$ can more effectively limit the radiation dose's impact on surrounding normal tissue. The increase in HI within Plan $_{VX}$ indicates a hotter boost inside the tumor. Despite minimal supporting clinical data, theoretically, with the same peripheral dose, a higher dose inside the tumor may translate to enhanced clinical efficacy in treating hypoxic tumors, thereby enhancing tumor control effects [6, 16]. Regarding the protection of OARs, $Plan_{VX}$ shows a trend of improvement in dose metrics for thoracic normal tissues, particularly demonstrating a significant advantage in reducing lung radiation exposure. These improvements are crucial for lowering the risk of treatment-related complications, effectively reducing long-term adverse reactions in patients, and improving quality of life. Notably, the performance of $Plan_{VX}$ in patients with multiple lesions is particularly outstanding, possibly due to its orthogonal bidirectional conformability and the capability to reduce leakage in large fields. This allows for more flexible and precise treatment planning in complex cases involving multiple tumor targets.

Several limitations remain. First, the small sample size limits statistical power and generalizability. Second, as a retrospective study, it is subject to selection and information biases. Third, the lack of long-term clinical outcomes—such as survival, tumor control, and quality of life—makes it difficult to assess the real-world benefits of VenusX, especially since both systems produced plans that met RTOG standards. Important clinical factors like immobilization, motion management, and IGRT were also not included. Additionally, the study used different dose calculation algorithms: collapsed cone convolution (CCC) for VenusX and Monte Carlo for Edge. These differences may partly explain the small dosimetric variations observed. Because the VenusX model was not compatible with the Pinnacle system at the time, both plans could not be recalculated in the same platform, limiting direct comparison. Future studies should include larger prospective cohorts, long-term follow-up, and standardized planning systems to better evaluate the clinical value of VenusX.

The introduction of the orthogonal dual-layer MLC accelerator represents a significant advancement in the field of radiation therapy. This study has demonstrated that, compared to single-layer MLC devices, it offers dosimetric advantages for SBRT treatment plans in both target areas and normal tissues, providing patients with more optimized treatment options. This is of great importance for improving patient survival rates and

quality of life. With the further development and application of orthogonal dual-layer MLC radiation therapy devices, it is expected that they will play an increasingly important role in the future practice of radiation therapy.

Conclusion

All treatment plans generated by Plan $_{VX}$ and the Plan $_{Edge}$ met the dosimetric criteria defined by the RTOG guidelines, indicating that both systems are capable of producing clinically acceptable SBRT plans. Plan VX demonstrated favorable values in terms of conformity index (CI), homogeneity index (HI), and gradient index (GI), with a trend toward reduced radiation exposure to critical organs, particularly the lungs. These dosimetric differences were more evident in complex multi-target cases. However, it is important to note that these findings reflect planning-level observations and do not establish definitive clinical superiority. The clinical significance of the observed differences remains uncertain and warrants further prospective investigation.

Abbreviations

SBRT	Stereotactic body radiation therapy
MLC	Multi-leaf collimator
OARs	Organs at risk
NSCLC	Non-small cell lung cancer
GTV	Gross tumor volume
ITV	Internal target volume
PTV	Planned target volume
TPS	Treatment planning system
HD	High definition
CCC	Collapsed cone convolution
MC	Monte Carlo
FMO	Fluence map optimization
CI	Conformity index
HI	Homogeneity index
GI	Gradient index
D_2	Dose received by the hottest 2%
D_{98}	Dose received by the coolest 98%
D_{50}	Dose received by 50% of the PTV
$D_{2\,cm}$	Maximum dose at 2 cm away from the PTV in all directions
V_5	Volume receiving at least 5 Gy
V_{20}	Volume receiving at least 20 Gy
D_{mean}	Mean dose
D_{max}	Maximum dose
BEV	Beam's eye view
RTOG	Radiation Therapy Oncology Group
FFF	Flattening filter free
SAD	Source to axis distance
CT	Computed tomography
4DCT	Four-dimensional computed tomography

Supplementary Information

The online version contains supplementary material available at https://doi.org/10.1186/s40001-025-02673-6.

Supplementary Material 1.

Acknowledgements
The authors thank the staff from Leitai Medical Corporation for their technical support.

Author contributions
Y.D and S.Z: data collection and analysis, interpretation of results, writing and revision of the manuscript. A.F: interpretation of results, review and editing. Q.K and Z.X: conception and design of the study, review and editing, approval of the final version.

Funding
Nurture projects for basic research of Shanghai Chest Hospital, Grant/Award Number: 2022YNTCQ09; Research and Progress in Precision Radiotherapy for Cancer Research Project, Grant/Award Number: J202305E038A04; National Natural Science Foundation Young Investigator Grant Program, Grant/Award Number: 82403785; General Program of National Natural Science Foundation of China, Grant/Award Number: 12375346; National Natural Science Foundation Young Investigator Grant Program, Grant/Award Number: 82203976.

Data availability
No datasets were generated or analysed during the current study.

Declarations

Ethics approval and consent to participate
The study is a retrospective study. When the study began, all selected patients signed informed consents and completed radiotherapy. Ethical standards and patients' confidentiality were ensured and in line with regulations of the local institutional review board and data safety laws. This study was approved by the Ethics Committee of Shanghai Chest Hospital (the committee's reference Number: KS24051).

Consent for publication
All authors of the manuscript have read and agreed to its content and are accountable for all aspects of the accuracy and integrity of the manuscript.

Competing interests
The authors declare no competing interests.

Received: 9 February 2025 Accepted: 9 May 2025
Published online: 27 May 2025

References

1. Zhu X, Li X, Gu H, et al. Radiation-induced lung injury patterns and the misdiagnosis after SBRT of lung cancer. Eur J Radiol. 2019;121: 108708.
2. Cao C, Wang D, Chung C, et al. A systematic review and meta-analysis of stereotactic body radiation therapy versus surgery for patients with non–small cell lung cancer. J Thorac Cardiovasc Surg. 2019;157(1):362-373.e8.
3. Cao Y, Chen H, Sahgal A, et al. The impact of local control on widespread progression and survival in oligometastasis-directed SBRT: results from a large international database. Radiother Oncol. 2023;186: 109769.
4. Duan Y, Feng A, Wang H, et al. Dosimetry and treatment efficiency of SBRT using TaiChiB radiotherapy system for two-lung lesions with one overlapping organs at risk. J Xray Sci Technol. 2024;32(2):379–94.
5. Duan Y, Cao H, Wu B, et al. Dosimetric comparison, treatment efficiency estimation, and biological evaluation of popular stereotactic radiosurgery options in treating single small brain metastasis. Front Oncol. 2021;11: 716152.
6. Duan Y, Lin Y, Wang H, et al. How does the gradient measure of the lung SBRT treatment plan depend on the tumor volume and shape? Front Oncol. 2021;11: 781302.
7. Miyasaka R, Cho S, Hiraoka T, et al. Investigation of Halcyon multi-leaf collimator model in Eclipse treatment planning system: a focus on the VMAT dose calculation with the Acuros XB algorithm. J Appl Clin Med Phys. 2022;23(3): e13519.
8. Panda S, Swamidas J, Chopra S, et al. Treatment planning comparison of volumetric modulated arc therapy employing a dual-layer stacked multi-leaf collimator and helical tomotherapy for cervix uteri. Radiat Oncol. 2020;15(1):22.

9. Videtic GM, Hu C, Singh AK, et al. A randomized phase 2 study comparing 2 stereotactic body radiation therapy schedules for medically inoperable patients with stage I peripheral non-small cell lung cancer: NRG Oncology RTOG 0915 (NCCTG N0927). Int J Radiat Oncol Biol Phys. 2015;93(4):757–64.
10. Radiation Therapy Oncology Group. RTOG 3502: a randomized phase II trial in patients with operable stage I non-small cell lung cancer: radical resection versus ablative stereotactic radiotherapy. http://www.rtog.org/ClinicalTrials/ProtocolTable/StudyDetails.aspx?study=3502. Acessed 1 May 2023.
11. Bezjak A, Paulus R, Gaspar LE, et al. Safety and efficacy of a five-fraction stereotactic body radiotherapy schedule for centrally located non-small-cell lung cancer: NRG Oncology/RTOG 0813 Trial. J Clin Oncol. 2019;37(15):1316–25.
12. Wu QJ, Wang Z, Kirkpatrick JP, et al. Impact of collimator leaf width and treatment technique on stereotactic radiosurgery and radiotherapy plans for intra- and extracranial lesions. Radiat Oncol. 2009;4:3.
13. van't Riet A, Mak AC, Moerland MA, Elders LH, van der Zee W. A conformation number to quantify the degree of conformality in brachytherapy and external beam irradiation: application to the prostate. Int J Radiat Oncol Biol Phys. 1997;37(3):731–6.
14. Huq M, Das I, Steinberg T, et al. A dosimetric comparison of various multileaf collimators. Phys Med Biol. 2002;47:N159–70.
15. Wang Q, Li Q, Wang Z, et al. Characterization of a novel VenusX orthogonal dual-layer multileaf collimator. J Appl Clin Med Phys. 2024;25(5):e14357.
16. Cao H, Xiao Z, Zhang Y, et al. Dosimetric comparisons of different hypofractionated stereotactic radiotherapy techniques in treating intracranial tumors > 3 cm in longest diameter. J Neurosurg. 2019;132(4):1024–32.

Publisher's Note